

pubs.acs.org/JPCC Article

Atomic Hydrogen Reactions of Alkanethiols on Au(111): Phase Transitions at Elevated Temperatures

David A. Turner, Catlin N. Schalk, and S. Alex Kandel*



Cite This: J. Phys. Chem. C 2020, 124, 7139-7143



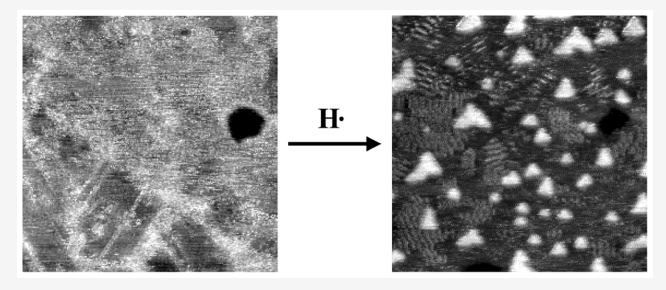
ACCESS

Metrics & More



Supporting Information

ABSTRACT: Scanning tunneling microscopy (STM) was used to observe the chemical transformations of an octanethiolate monolayer on Au(111) exposed to gas-phase atomic hydrogen at 27 °C. Reaction begins with the steady conversion of the close-packed ϕ phase to the high-density, liquid-like ϵ phase. Following this step is a rapid event in which both ϕ and ϵ disappear from the surface and are replaced with low-density striped-phase structures. The ϵ phase, which does not form at room temperature, leads to this more complex reaction behavior. Experimental observations are reproduced by a simple set of kinetic equations describing the



transformations between phases and the relative reactivity of molecules in each phase. Reaction kinetics had previously been attributed to enhanced reactivity near defect sites; with the phase transformation model, no such enhancement is necessary. The reaction rate of monolayers formed from 8-mercapto-1-octanol confirms this proposal, as the much higher density of defects in these monolayers does not cause significant changes in the reaction.

■ INTRODUCTION

There has been significant interest in how alkanethiolate monolayers change when exposed to energetic environments that include reactive species such as hyperthermal rare-gas atoms, atomic radicals, and ions. ¹⁻¹² Hydrogen-atom reactions with alkanethiolates have received particular attention, starting with the work of Fairbrother and co-workers in 2007, who showed that there are two pathways for the reaction: (1) hydrogenation of the sulfur—gold bond at the monolayer—substrate interface, leading to the desorption of the molecule from the surface, and (2) hydrogen abstraction from the hydrocarbon backbone, producing surface radicals that eventually lead to cross-linking between neighboring carbon chains. ¹³ For short-chain monolayers (≤12 carbon atoms) the first reaction dominates and hydrogen-atom exposure eventually leads to complete removal of organics from the surface.

In this manuscript, we discuss the reaction of an octanethiolate SAM with atomic hydrogen, and we revisit one of the earlier conclusions from our laboratory, that defect sites in alkanethiolate monolayers are substantially more reactive than close-packed sites. ¹⁴ This conclusion was based on the observation by Kautz et al. that the reaction rate of octanethiolate SAMs with atomic hydrogen accelerated with hydrogen exposure. This was interpreted as the result of defect sites being more reactive than close-packed areas; as the monolayer reacts, additional defect sites are formed, leading to an increase in reaction rate. A different interpretation was recently offered by Sayler et al., who demonstrated the same accelerating rate for a range of alkanethiolate chain lengths (8–11 carbon atoms). ¹⁵ The experimental data in that study were

fit using kinetic equations that did not assume a different reaction rate for defect sites but instead described the reaction as occurring in two steps. One step involves a slow reaction of hydrogen with close-packed areas, and the other step is a fast reaction between hydrogen and a low-density striped phase. With this model, the observed accelerating reaction rate is due to the progressive conversion of the close-packed monolayer to a low-density striped phase, which then reacts with hydrogen at a substantially greater rate. 15

The phase diagram (depending on coverage and temperature) of alkanethiolate monolayers is complex. $^{16-19}$ Our current study is of the reaction of octanethiolate monolayers with atomic hydrogen at slightly elevated (27 °C) temperature, where striped and close-packed phases coexist with an intermediate-density liquid phase (ϵ) that is not seen at room temperature. Following Sayler et al., we are able to describe the complex reaction process in terms of the phase transformations that occur as alkanethiolates are removed from the surface. The formation of the liquid phase results in more complicated reaction kinetics, which nonetheless can be described qualitatively with a combination of five reaction steps.

Received: November 21, 2019 Revised: March 10, 2020 Published: March 10, 2020



Additionally, we report on the reaction of hydrogen atoms with monolayers formed from 8-mercapto-1-octanol. While we would not expect this molecule to react differently compared to an alkanethiolate, the monolayers formed have substantially less order and therefore a much higher density of defect sites. We find that the greater number of defects does not qualitatively or quantitatively affect the reaction rate and take this as evidence that it is the phase transformations and not defect creation that are responsible for the accelerating reaction rates observed for hydrogen-atom reaction with alkanethiolate SAMs.

■ EXPERIMENTAL SECTION

Experiments are performed using a home-built, UHV scanning tunneling microscope (STM) with the same scanner assembly described by Jobbins et al. An Oxford Scientific OS-Crack thermal gas cracker is used to produce hydrogen atoms. Au(111)-on-mica substrates (Keysight Technologies) are prepared by hydrogen flame annealing under ambient conditions. The annealed substrates are then transferred into a 20 mL vial along with a small tube of 1-octanethiol and the vial is closed off. 1-Octanethiol (Millipore Sigma, \geq 98.5%), is used without any further preparation, and the samples are placed in a 65 °C oven for at least 18 h to vapor deposit. Samples are allowed to cool to room temperature before being removed from the vial.

A tube containing a 10 mM 8-mercapto-1-octanol (Millipore Sigma, 98%) in acetonitrile solution is placed in a 20 mL vial with an annealed substrate. The vial is closed and then left at room temperature for a week. Both 1-octanethiol and 8-mercapto-1-octanol samples are transferred into the vacuum chamber (base pressure 10^{-9} Torr) without any further treatment. Structures for both molecules can be found in Figure 1. STM images are acquired with a mechanically cut Pt/ Ir tip in constant current mode at 27 °C with a tunneling current of 100-200 pA and a sample bias of +0.5 V.



Figure 1. Chemical structures of (a) 1-octanethiol and (b) 8-mercapto-1-octanol.

Because the tip is retracted during a hydrogen dose, an area with recognizable features is chosen for experiments. Surface landmarks ensure that the same area is being monitored throughout the experiment, and gradual changes can be observed. Molecular hydrogen is introduced to the chamber to achieve a base pressure of 10⁻⁶ Torr and passed through a heated tungsten capillary to create hydrogen atoms. During a hydrogen atom dose, the STM tip is retracted, and the hydrogen cracker capillary is heated to 1800-2000 K. A mechanical shutter blocking the exit of the cracker is moved to allow hydrogen atoms to reach the sample. After 10 s of exposure, the shutter is moved back in place and the tip is moved back to the tunneling position for imaging. This process is repeated until no monolayer remains on the surface. The hydrogen flux is not measured directly but is calculated to be on the order of 10¹⁴ hydrogen atoms per cm⁻² per second. With a cracking efficiency of 6-27% and the calculated flux, the amount of hydrogen atoms colliding with an octanethiol molecule is approximately 2-8 atoms per 10 s.

STM images in Figure 2 and Figure 5c are filtered by removing a constant offset from each scan line. This subtraction was masked to avoid pit and island defects, and fit over multiple terraces in Figure 5c.²²

■ RESULTS AND DISCUSSION

1-Octanethiol. The 1-octanethiol surface begins with molecules packed in the ϕ phase. With even a small hydrogen dose, the ϵ and ϕ phases can be found coexisting on the surface; this is shown in the Supporting Information in Figure S1. While much of the surface remains covered with the close-packed, standing-up ϕ phase, a portion of it has converted to the ϵ phase. ϵ was described by Poirier et al. as a liquid-like, disordered phase with medium-to-high coverage that is present above room temperature. ^{16–19} Here, areas of ϵ are characterized by a different topographic height, a lack of observable molecular structure, and a noisiness in imaging that likely results from the mobile nature of the molecules. A line scan of the difference between ϕ and ϵ is given in Figure S2.

An example surface measured over the course of the reaction is shown in Figure 2. This sample is representative of six experiments where the same observations are made of a steady conversion of ϕ to ϵ followed by the sudden transformation to the striped phase and the appearance of gold islands. Initial changes are relatively small, accumulating as more of the surface area converts from ϕ (packing density 21.6 Å²/ molecule) to ϵ (packing density between 21.6-54.0 Å²/ molecule). 16 Following this, one additional 10 s dose results in complete removal of both ϕ and ϵ phases, the appearance of striped phases (packing densities vary between 54.0-82.8 Å²/ molecule)¹⁶ covering some (but not all) of the surface, and the growth of gold islands. While it is well reported that islands form from the gold adatoms that are left behind upon monolayer removal, these islands typically form gradually as molecules desorb from the surface.²³ The sudden appearance of gold islands has not previously been reported.

As molecules in the close-packed ϕ phase react with atomic hydrogen, they are removed from the surface via hydrogenation of the gold—sulfur bond, 13 leaving behind vacancies in the monolayer. Sayler et al. 15 observed that at 22.0 °C, vacancy formation led to the conversion of ϕ to lying-down, striped phases. In our experiments, the slightly elevated temperature (27 °C) is responsible for a significant change in the monolayer reaction dynamics. The driving factor in changing the path of this reaction is the movement into a higher-temperature region of the alkanethiolate monolayer phase diagram. As a result, the formation of vacancies allows molecules in the ϕ phase to instead relax and form the ϵ phase, which is not present at room temperature.

The sudden transformation of the surface to the striped phase (and accompanying formation of adatoms) is the expected result of the intermediate formation of the ϵ phase. We propose a simple model describing the reaction kinetics in which we describe surface transformation as occurring through five distinct processes:

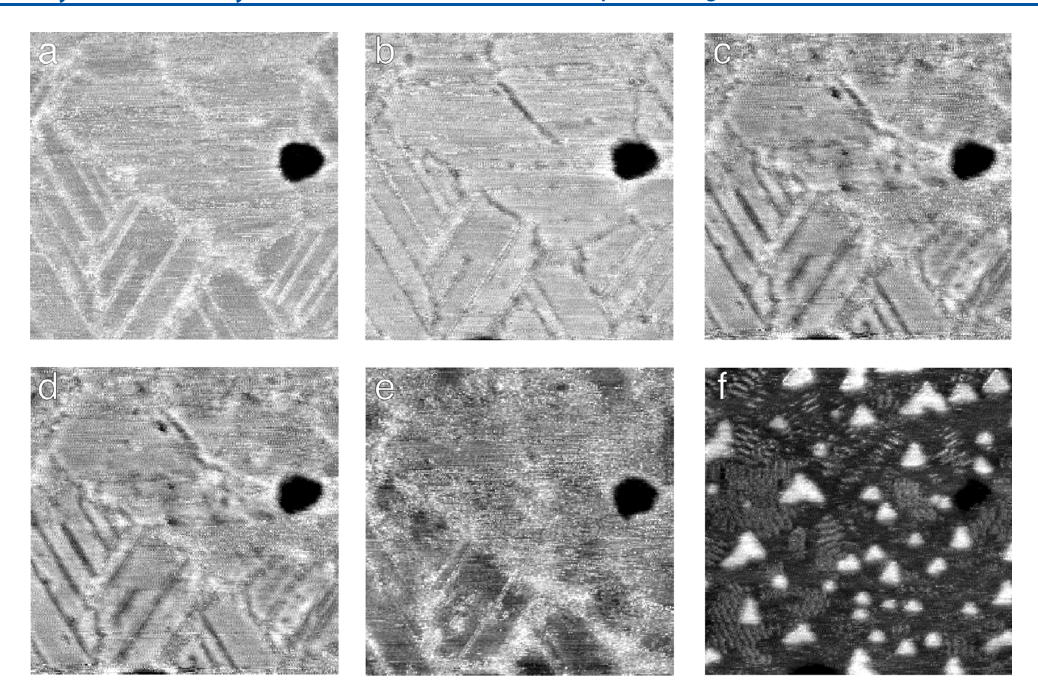


Figure 2. $61.8 \text{ nm} \times 67.4 \text{ nm}$ of the same area of the sample shown over time: (a) 20 s exposure, (b) 30 s exposure, (c) 40 s exposure, (d) 70 s exposure, (e) 100 s exposure, (f) 110 s exposure where there is a sudden island event.

$$\begin{array}{lll} \phi \rightarrow * & k_1 & \text{(small)} \\ \phi + * \rightarrow 2\epsilon & k_2 & \text{(very large)} \\ \epsilon + * \rightarrow 2S & k_3 & \text{(very large)} \\ \epsilon \rightarrow * & k_4 & \text{(small)} \\ S \rightarrow * & k_5 & \text{(large)} \end{array}$$

The first reaction is the formation of vacancies (denoted *) from the combination of atomic hydrogen with a ϕ region on the surface. Following Sayler et al., 15 we expect this to be a slow process, since it is difficult for the hydrogen to access the gold—sulfur bonds in close-packed regions; k_1 is small. The second and third reactions are the phase transformations, from ϕ to ϵ and from ϵ to the striped phase, ϵ . Changing phase requires the presence of a vacancy site, but once these sites are available we expect that the transformation is very fast; accordingly, k_2 and k_3 are taken to be very large. The fourth and fifth reactions are the removal of ϵ and ϵ from the surface; we assume that ϵ will be comparable in magnitude to (or perhaps slightly larger than) ϵ sayler et al. 15 tells us that ϵ is substantially larger than ϵ to the surface and ϵ sayler et al. 15 tells us that ϵ is substantially larger than ϵ to the surface;

The reactions are balanced so that the number of sites, occupied by molecules in any of the three phases or unoccupied as vacancies, stays the same throughout the reaction. This is a simplifying assumption that is unlikely to exactly match reality; for example, we would expect that several vacancies would need to be created to allow the transformation of a single ϕ molecule into the S phase.

The reactions described above result in the following kinetic equations:

$$\begin{split} \frac{\partial[\phi]}{\partial t} &= -k_1[\phi] - k_2[\phi][*] \\ \frac{\partial[\epsilon]}{\partial t} &= 2k_2[\phi][*] - k_3[\epsilon][*] - k_4[\epsilon] \\ \frac{\partial[S]}{\partial t} &= 2k_3[\epsilon][*] - k_5[S] \\ \frac{\partial[*]}{\partial t} &= k_1[\phi] - k_2[\phi][*] - k_3[\epsilon][*] + k_4[\epsilon] + k_5[S] \end{split}$$

Figure 3 shows the numerical integration of the five rate equations, and the qualitative features that result—especially the sudden drop in both ϕ and ϵ coverage concomitant with the appearance of the striped phase—are a good match to the experimental observations.

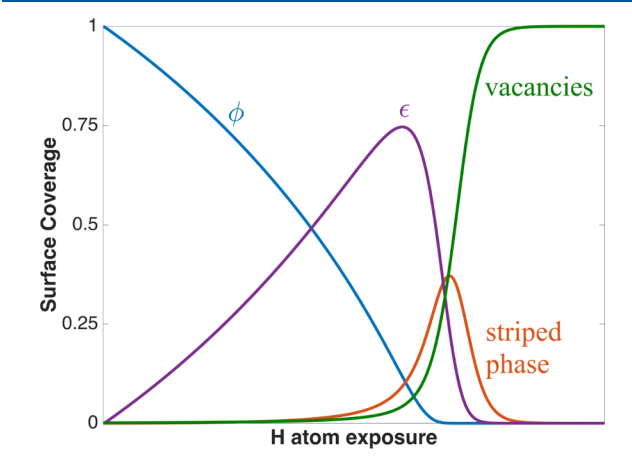


Figure 3. Coverage versus time plot representing the different species present on the 1-octanethiol surface. The blue line shows ϕ , purple ϵ , orange striped phase, green vacancies. Values of (arbitrarily scaled) rate constants are $k_1 = 0.0001$, $k_2 = 0.1$, $k_3 = 0.02$, $k_4 = 0.0005$, and $k_5 = 0.01$.

8-Mercapto-1-octanol. Further insight is gained by comparing the reactions of octanethiolate monolayers with the corresponding OH-terminated SAM, formed from 8-mercapto-1-octanol. Because the tail group is not bulky, we expect it to have little effect on the reaction of H atoms with the sulfur headgroup. Furthermore, we do not expect direct reactions between H atoms and the OH tail group; the O–H bond is significantly stronger than the H–H bond, meaning that any incoming atomic hydrogen would not have appropriate energy to abstract a hydrogen from the OH tail group. The major difference between the OH- and CH₃-terminated SAMs is their packing order: while the CH₃-terminated SAMs have large ϕ domains separated by defects, the OH-terminated SAMs have no evident ϕ domains and are almost entirely disorganized. This can be seen in Figure 4.

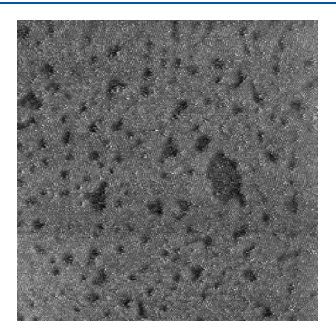


Figure 4. 75.0 nm \times 75.0 nm STM image of 7 day room temperature vapor deposited 8-mercapto-1-octanol on Au(111).

Kautz et al. predicts that molecules near defects will react substantially faster than close-packed molecules; if this is the case, we would see a large increase in reactivity for the OH-terminated SAM. However, despite the increased amount of defects found on this surface, monolayers formed from 8-mercapto-1-octanol react similarly to 1-octanethiolate SAMs in that the surface reaction is barely perceptible until a single event that forms striped-phase molecules and adatoms; the timing of this event is similar for both 8-mercapto-1-octanol and octanethiol-derived SAMs. This progression can be seen in Figure 5.

CONCLUSIONS

A defining characteristic of the reaction of hydrogen atoms with short-chain alkanethiolate SAMs is a rate that accelerates as the reaction proceeds. This was observed for octanethiolate SAMs by Kautz et al.¹⁴ and more recently for octanethiolate

through undecanethiolate SAMs by Sayler et al. ¹⁵ The latter study makes a strong case that the acceleration is the result of a much higher reaction rate for low-density, striped-phase thiolates, which constitute more and more of the surface as the reaction proceeds. This latter interpretation appears to apply well to the results presented here, which show the reaction of octanethiolate SAMs at a slightly elevated temperature. We observe slow conversion of the close-packed ϕ phase to the liquid-like ϵ phase, followed by sudden conversion of both to the low-density stripe phase. This is a more complex process that nonetheless can be explained qualitatively as the result of phase transformation, using phase-dependent reaction rates.

The explanation offered by Kautz et al. ¹⁴ is that the acceleration of the reaction is caused by differentially greater reactivity at defect sites, which also increases as the reaction progresses. This hypothesis is not easily extended to cover the more complex, higher-temperature results presented here. Defect sites may be more reactive, but the extent to which they are remains unknown. Furthermore, the comparison of CH₃-terminated and OH-terminated SAMs shows they are quite similar with respect to H atom reaction, despite a vastly greater density of defect sites in the OH-terminated monolayer.

Finally, the data here show that gold islands appear concurrently with striped-phase formation. It is well-known that formation of the ϕ phase reconstructs the gold surface, and that additional gold atoms (relative to a bulk-terminated substrate) are freed up upon removal of the monolayer. It is clear from the current results that both the ϕ and ϵ phases involve a reconstruction at the sulfur—gold interface, while the striped phase does not.

ASSOCIATED CONTENT

Supporting Information

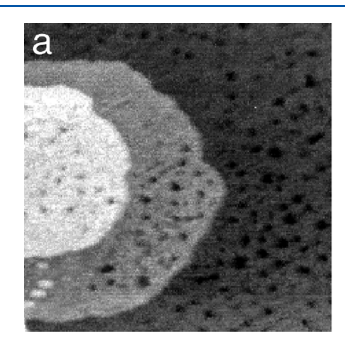
The Supporting Information is available free of charge at https://pubs.acs.org/doi/10.1021/acs.jpcc.9b10914.

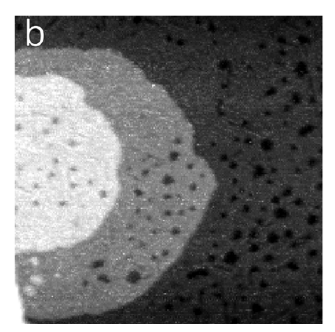
STM images of phases coexistence, line scans, surface coverage vs H exposure time, and image masks (PDF)

AUTHOR INFORMATION

Corresponding Author

S. Alex Kandel — Department of Chemistry and Biochemistry, University of Notre Dame, Notre Dame, Indiana 46556, United States; Occid.org/0000-0001-8191-1073; Email: skandel@nd.edu





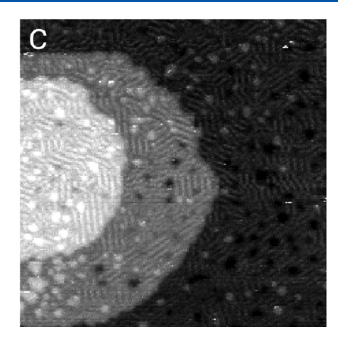


Figure 5. 87.2 nm × 92.6 nm STM image of the same area of an 8-mercapto-1-octanol surface at (a) 50 s hydrogen exposure, (b) 100 s hydrogen exposure, and (c) 110 s hydrogen exposure where a similar adatom and striped phase event occurred as the 1-octanethiol surface.

Authors

- David A. Turner Department of Chemistry and Biochemistry, University of Notre Dame, Notre Dame, Indiana 46556, United States
- Catlin N. Schalk Department of Chemistry and Biochemistry, University of Notre Dame, Notre Dame, Indiana 46556, United States

Complete contact information is available at: https://pubs.acs.org/10.1021/acs.jpcc.9b10914

Notes

The authors declare no competing financial interest.

ACKNOWLEDGMENTS

Support for this work has been provided by the National Science Foundation (NSF CHE-1807313).

REFERENCES

- (1) Isa, N.; Gibson, K. D.; Yan, T.; Hase, W.; Sibener, S. J. Experimental and simulation study of neon collision dynamics with a 1-decanethiol monolayer. *J. Chem. Phys.* **2004**, *120*, 2417–2433.
- (2) Li, W.; Langlois, G. G.; Kautz, N. A.; Sibener, S. J. Formation of stabilized ketene intermediates in the reaction of O(³P) with oligo(phenylene ethynylene) thiolate self-assembled monolayers on Au(111). *J. Phys. Chem. C* **2014**, *118*, 15846–15852.
- (3) Yuan, H.; Gibson, K. D.; Li, W.; Sibener, S. J. Modification of alkanethiolate monolayers by O(³P) atomic oxygen: Effect of chain length and surface temperature. *J. Phys. Chem. B* **2013**, *117*, 4381–4389.
- (4) Gibson, K. D.; Isa, N.; Sibener, S. J. Experiments and simulations of hyperthermal Xe interacting with an ordered 1-decanethiol/Au(111) monolayer: Penetration followed by high-energy, directed ejection. *J. Phys. Chem. A* **2006**, *110*, 1469–1477.
- (5) Fogarty, D. P.; Kautz, N. A.; Alex Kandel, S. Collision-induced diffusion and vacancy migration in alkanethiol monolayers on Au(111). *Surf. Sci.* **2007**, *601*, 2117–2124.
- (6) Day, B. S.; Shuler, S. F.; Ducre, A.; Morris, J. R. The dynamics of gas-surface energy exchange in collisions of Ar atoms with ω-functionalized self-assembled monolayers. *J. Chem. Phys.* **2003**, *119*, 8084–8096.
- (7) Esplandiu, M. J.; Carot, M. L.; Cometto, F. P.; MacAgno, V. A.; Patrito, E. M. Electrochemical STM investigation of 1,8-octanedithiol monolayers on Au(1 1 1).: Experimental and theoretical study. *Surf. Sci.* **2006**, *600*, 155–172.
- (8) Carot, M. L.; Esplandiu, M. J.; Cometto, F. P.; Patrito, E. M.; MacAgno, V. A. Reactivity of 1,8-octanedithiol monolayers on Au(1 1): Experimental and theoretical investigation. *J. Electroanal. Chem.* **2005**, *579*, 13–23.
- (9) Alexander, W. A.; Day, B. S.; Moore, H. J.; Lee, T. R.; Morris, J. R.; Troya, D. Experimental and theoretical studies of the effect of mass on the dynamics of gas/organic-surface energy transfer. *J. Chem. Phys.* **2008**, 128, 014713.
- (10) Lohr, J. R.; Day, B. S.; Morris, J. R. Scattering, accommodation, and trapping of HCl in collisions with a hydroxylated self-assembled monolayer. *J. Phys. Chem. B* **2005**, *109*, 15469–15475.
- (11) Alexander, W. A.; Morris, J. R.; Troya, D. Theoretical study of the stereodynamics of CO collisions with CH 3- and CF 3-terminated alkanethiolate self-assembled monolayers'a. *J. Phys. Chem. A* **2009**, 113, 4155–4167.
- (12) Alexander, W. A.; Troya, D. Theoretical study of the dynamics of collisions between HCl and ω -hydroxylated alkanethiol self-assembled monolayers. *J. Phys. Chem. C* **2011**, *115*, 2273–2283.
- (13) Gorham, J.; Smith, B.; Fairbrother, D. H. Modification of alkanethiolate self-assembled monolayers by atomic hydrogen: Influence of alkyl chain length. *J. Phys. Chem. C* **2007**, *111*, 374–382.

- (14) Kautz, N. A.; Kandel, S. A. Reactivity of self-assembled monolayers: Local surface environment determines monolayer erosion rates. *J. Phys. Chem. C* **2012**, *116*, 4725–4731.
- (15) Sayler, J. D.; Brown, S.; Sibener, S. J. Chain-length-dependent reactivity of alkanethiolate self-assembled monolayers with atomic hydrogen. *J. Phys. Chem. C* **2019**, *123*, 26932–26938.
- (16) Poirier, G. E.; Fitts, W. P.; White, J. M. Two-dimensional phase diagram of decanethiol on Au(111). *Langmuir* **2001**, *17*, 1176–1183.
- (17) Poirier, G. E.; Pylant, E. D. The self-assembly mechanism of alkanethiols on Au(111). Science 1996, 272, 1145–1148.
- (18) Poirier, G. E. Mechanism of formation of Au vacancy islands in alkanethiol monolayers on Au(111). *Langmuir* **1997**, *13*, 2019–2026.
- (19) Poirier, G. E. Characterization of organosulfur molecular monolayers on Au(111) using scanning tunneling microscopy. *Chem. Rev.* **1997**, *97*, 1117–1127.
- (20) Jobbins, M. M.; Agostino, C. J.; Michel, J. D.; Gans, A. R.; Kandel, S. A. Compact, single-tube scanning tunneling microscope with thermoelectric cooling. *Rev. Sci. Instrum.* **2013**, *84*, 103708.
- (21) Deering, A. L.; Van Lue, S. M.; Kandel, S. A. Ambient-pressure vapor deposition of octanethiol self-assembled monolayers. *Langmuir* **2005**, 21, 10260–10263.
- (22) Fogarty, D. P.; Deering, A. L.; Guo, S.; Wei, Z.; Kautz, N. A.; Kandel, S. A. Minimizing image-processing artifacts in scanning tunneling microscopy using linear-regression fitting. *Rev. Sci. Instrum.* **2006**, 77, 126104.
- (23) Kautz, N. A.; Kandel, S. A. Alkanethiol/Au(111) self-assembled monolayers contain gold adatoms: Scanning tunneling microscopy before and after reaction with atomic hydrogen. *J. Am. Chem. Soc.* **2008**, *130*, 6908–6909.